

Interactive comment on “Chemistry and deposition in the Model of Atmospheric composition at Global and Regional scales using Inversion Techniques for Trace gas Emissions (MAGRITTEv1.0). Part A. Chemical mechanism” by Jean-François Müller et al.

Jean-François Müller et al.

jean-francois.muller@aeronomie.be

Received and published: 17 April 2019

Reply to Anonymous Referee #1

We thank the referee for their comments and respond to the points raised below.

C1

These concerns are detailed below in reference to the locations in the manuscript at which they appear, but briefly, they generally include the effects of specific (particularly the more poorly- understood) isoprene oxidation pathways on model outcomes along with the treatment of SOA and monoterpenes. The authors acknowledge that all of these aspects come with substantial uncertainty, but without any quantification of that uncertainty in the model, it is difficult for the reader to know how much proverbial stock to put into simulation results. It is perfectly reasonable that the model is not intended to provide detailed accounting of global biogenic SOA formation or the effects of terpene oxidation, but more discussion is needed regarding the limitations of these aspects of the model. For example, while some SOA formation pathways are included in the model (e.g. IEPOX reactive uptake), others are only mentioned as the likely sinks of isoprene oxidation products, without any physical reaction parameterized in the model (e.g. dinitrates and the hydroperoxy-epoxides from D'Ambro et al. (2017)). A modeler could assume that these products form SOA immediately with a 100% yield, but because some of the low-volatility species that lead to SOA formation would likely also have high deposition velocities, this could overestimate the SOA yield. How do these (and other) sources of uncertainty in the important results from this mechanism (e.g. HOx budgets, organic acid budgets, SOA) manifest themselves in a global model, and what should the reader take away regarding the potential for bias and error in simulating the overall effects of isoprene's oxidation on the chemistry of the global troposphere?

The Reviewer is of course correct that the hydroperoxy-epoxides from D'Ambro et al. (2017) are not entirely converted to SOA. We now provide more discussion on SOA formation in the global modeling results Section (Sect. 4.2). We provide quantitative estimates of the main different pathways and their impact on the model results, as discussed further below (see response to Referee comment on DHHEPOX and SOA, p26 L14). In any case, we want to remind the Reviewer that the current focus of our mechanism is not on SOA formation.

C2

On the issue of uncertainties: As discussed further below, uncertainties are plenty, and not confined to a single specific part of the mechanism. It is very difficult, and, to our view, out of scope of the present study, to go through every significant uncertainty in the mechanism and quantify their potential consequences. As required by the Reviewer, we provide some estimation of the potential impact of uncertainties related to the effect of SOA formation and wet/dry deposition on the formaldehyde production from monoterpene oxidation. Following the suggestion of Reviewer #2, we also present a box model comparison of the MAGRITTE, Caltech and MCM mechanisms, which will help readers to better evaluate in which conditions and for which species the mechanisms present important discrepancies.

p4 L17: 5% can still be a lot of carbon for isoprene! Other pathways that also account for less than 5% of the total carbon from isoprene are included in this mechanism. Are there other reasons the bimolecular reactions of the delta-hydroxyperoxy radicals are excluded? Do we have any knowledge of how much this simplification might bias the results of simulations using this model?

We now include these pathways in the mechanism. We have added a new subsection detailing this chemistry (Section 2.1.3 Traditional chemistry of the initial δ -OH peroxy radicals). New model compounds are added: the C_5 hydroxycarbonyls, HALD1 and HALD2, and the δ -hydroxynitrate ISOPANO3 ($HOCH_2-C(CH_3)=CH-CH_2ONO_2$), not lumped anymore with ISOPCNO3 ($HOCH_2-CH=C(CH_3)-CH_2ONO_2$).

L25 & the rest of this section: the discussion of remaining uncertainties in this mechanism pathway is welcome, but given the important effects of this pathway on simulation results (e.g. as a source of HOx radicals in the otherwise HOx-consuming mechanism), it would be useful to provide the reader with some discussion (perhaps in the model results section) of how these uncertainties manifest themselves in the model. What range of possible HOx recycling rates would be compatible with what is currently

C3

known about this part of the mechanism? Given the uncertainties, can the boundary layer OH change due to this mechanistic pathway (Figure 3) be considered a bound or a best guess, and is the uncertainty on that at all quantifiable?

This part of the chemical mechanism has undergone major changes. As now discussed in great detail in a new subsection (Section 2.1.2), which we provide *in extenso* at the end of this Authors' response, the quantitative product distribution from the 1,6 H-shift of the Z - δ -OH-peroxys is adopted from the recent experimental study of Berndt et al. (2019), supported and complemented by computational results of the LIM1 paper (Peeters et al., 2014). A crucial point is that, contrary to speculative suggestion in the LIM1 paper, the Z - E isomerism of the transition states is conserved in the allylic-radical products and in the resulting peroxy. The implications are detailed in the new Section 2.1.2. Both theoretical expectation and experimental results imply a high HPALD yield (ca. 75%), whereas hydroperoxy carbonyl epoxides (HPCE, 15%) and the dihydroperoxycarbonyl peroxy (DIHPCARPs, 10%) make up the rest. The further chemistry of HPCE and DIHPCARPs is also discussed in this Section. The MAGRITTE mechanism (v1.1) has been revised to accommodate these important changes, including new model compounds (HPCE as well as several compounds resulting from the further chemistry of HPCE and DIHPCARPs). Note that the high HPALD yield is also comforted by the model evaluation against SEAC⁴RS measurements at the CIMS mass corresponding to HPALD (see our response to the last Reviewer comment).

In consequence, the product distribution of the 1,6 H-shift of the Z - δ -OH-peroxys is probably not the most important source of uncertainty in the overall mechanism. Uncertainties remain important, but are not confined to this part of the mechanism. It is therefore very difficult to go through every significant source of uncertainty in the mechanism and quantify its potential consequences. Following the suggestion of Reviewer #2, we now present a box model comparison of the MAGRITTE, Caltech and MCM mechanisms, which will help readers to better evaluate in which conditions and for which species the mechanisms present important discrepancies. For example, sig-

C4

nificant differences are found for OH at low-NOx, with Caltech predicting higher concentrations by about 30% higher than the other mechanisms. For the most part, the differences can be traced back to assumptions regarding the isomerization of *Z*- δ -OH-peroxys and the photolysis of hydroperoxycarbonyls. Although the MAGRITTE results should be viewed as state-of-the-art, more work is needed to confirm and refine the assumptions made in our study. An extensive review of the uncertainties and their potential consequences is out of scope of the present study.

p9 L15: Fig 1 doesn't show latitude dependence as claimed here. It also convolutes the pressure and temperature dependences in a way that might not be useful for readers who would like to extrapolate for conditions other than 40 degrees N in January and July. I would suggest either clarifying some of the details of these conditions (e.g. add side plots of temp and pressure vs. altitude in January and July, or separate this into plots of yield vs. temp and yield vs. pressure).

The yields are now shown as functions of pressure instead of altitude, and the plot now includes a side plot of temperature vs. pressure.

p9 L19: "such" should be "this". Also, Wennberg et al. (2018) does not show that this procedure inherently overestimates most measured nitrate yields, though it does suggest that this equation provides yields that seem excessive for dinitrates. Instead it goes off the recommendation of Teng et al. (2017), which explicitly says that this provides a better estimate than just $n=\#C$, and improves this with a structure-activity-relationship-style modification.

We now use the parameterization of Wennberg et al. (2018) for the calculation of RONO₂ yields. We have updated Section 2.6 (Peroxy radical reactions with NO and HO₂) accordingly.

p26 L3: what is "isoprene-OH segregation"? What was the logic behind the 7% minor

C5

*addition channel, and behind including those but not the *E/Z*-delta bimolecular products?*

As explained above, we have now included the *E/Z*- δ -OH-peroxy bimolecular reactions and products. The "isoprene-OH segregation" effect results from incomplete mixing within a model grid cell and unresolved anti-correlation between isoprene and OH (due to their mutual reaction). The 10% reduction estimate is consistent with the results of Pugh et al. (2011) based on measurements in a tropical forest in Borneo.

p26 L10: if you include the description of Y(Arey) in the table heading, you don't need it in the footnote; I think the table heading should be shorter and this could be a footnote. Also, don't all the scaling factors >1 suggest that $N=\#$ heavy atoms would've been better than $N=\#C$?

As suggested by the Reviewer, we shortened the table heading. As noted above, we now use the organic nitrate parameterization by Wennberg et al. (2018).

p26 L11: define "room conditions" (this also comes up on p27 L4 & 13, p31 L15, 18 & 25, p32 L20, and p41 L34.

Done as requested.

p26 L14: Does this inherently assume that all DHHEPOX is lost to aerosols? Are there any estimates of the OH reaction coefficient or uptake coefficient of DHHEPOX that might put this assumption in context, or provide the reader with some idea as to the uncertainty on this assumption? What fraction of carbon is lost to this pathway under atmospheric conditions (and to other dead-end pathways assumed to either deposit or partition to aerosols, e.g. the dinitrates discussed in N9), and what is the resulting contribution to aerosol compared to other pathways (e.g. IEPOX)?

C6

The Reviewer is correct that DHHEPOX is not entirely lost to aerosols. We have updated the text (Note N6) as follows: "The further chemistry of the dihydroxy hydroperoxy epoxide resulting from this isomerisation, DHHEPOX, is not considered. Its saturation vapour pressure is estimated to be of the order of $3 \cdot 10^{-9}$ atm at 298 K using a group contribution method (Compernolle et al., 2011), i.e. three orders of magnitude lower than the estimated vapour pressure of β -IEPOX ($3 \cdot 10^{-6}$ atm). The Henry's law constant (HLC) of DHHEPOX estimated as described in Muller et al. (2018) is equal to $\sim 3 \cdot 10^9$ M atm $^{-1}$ at 298 K, almost three orders above the estimated value for IEPOX. DHHEPOX is therefore very probably more soluble and prone to loss by deposition or SOA formation than IEPOX, which has been shown to deposit very rapidly on vegetation (Nguyen et al., 2015b) and to be a prominent SOA precursor (Surratt et al., 2010). Furthermore, the products of the oxidation of DHHEPOX by OH (at a rate estimated at $\sim 2.1 \cdot 10^{-11}$ molec. $^{-1}$ cm 3 s $^{-1}$) are also expected to consist, for the most part, of highly oxygenated products prone to deposition and heterogeneous uptake. "

We thank the Reviewer for the interesting question on SOA formation. We inserted a new paragraph at the end of Section 4.2: "Although SOA is not a focus of this study, SOA formation processes are included in the model. The largest source of SOA is the uptake of IEPOX, with a global flux (49 Tg or 25 TgC yr $^{-1}$) of magnitude similar to previous model estimates, of the order of 40 Tg yr $^{-1}$ (Lin et al., 2012; Stadtler et al., 2018). These estimates are very uncertain, since the reactive uptake parameterization used in models ignores the complexity of SOA formation which involves the partitioning of semi-volatile compounds and chemical transformations in the gaseous and particulate phases (D'Ambro et al., 2019). Glyoxal is another well-identified source of SOA, amounting to 10 Tg yr $^{-1}$ globally (4.3 TgC yr $^{-1}$), also well in the range of previous estimations (6-14 Tg yr $^{-1}$) (Fu et al., 2008; Stavrakou et al., 2009b; Lin et al., 2012). The dihydroxy dihydroperoxides (ISOP(OOH) $_2$) formed from the oxidation of ISOPPOOH by OH were recently estimated to be a dominant source of SOA (Stadtler et al., 2018); in our mechanism, these compounds are ignored since their yields are believed to be negligible in atmospheric conditions (D'Ambro et al., 2017). The major

C7

non-IEPOX products of OH-addition to ISOPPOOH are dihydroxy hydroperoxy epoxides (DHHEPOX), also believed to form SOA as discussed above (Note N6). Their global production in the model amounts to 30 Tg yr $^{-1}$ (12 TgC yr $^{-1}$). Assuming that their reactive uptake is as effective as for IEPOX, and neglecting gas-phase oxidation by OH (which generates other low-volatility compounds also expected to form SOA), we estimate with the model that SOA formation accounts for two-thirds of the sink of DHHEPOX (i.e. 20 Tg yr $^{-1}$), whereas dry/wet deposition makes up the rest. If confirmed, this would make DHHEPOX the second-largest contribution to isoprene SOA.

Other SOA formation pathways are implied, but not explicitly represented by the MAGRITTE mechanism, such as the hydrolysis of dihydroxy dinitrates (Note N12) and dihydroxy hydroperoxy nitrates (Note N13). The hydrolysis products, nitroxy- and hydroperoxy-triols are expected to be of very low volatility and remain mostly in the aerosol phase, as their vapour pressures (Compernolle et al., 2011) are estimated to be very low. Those triols represent only a minor contribution to the global SOA budget, however, as their estimated global production is ~ 3 Tg yr $^{-1}$ (1.2 TgC yr $^{-1}$). "

p26 L22: despite this being "well known" I think it deserves a citation, and more support than that the "majority" of exothermicity is alternately directed, making it "appear unlikely". It is difficult from reading this footnote to tell what is conjecture and what has experimental evidence to support the pathways used. The language generally implies certainty, but the lack of citations suggests that it is conjecture.

We have modified this part of the Note as follows: "Abstraction of hydroperoxide-H (75%) and of hydroxy- α -H (25%) (Wennberg et al., 2018). The latter leads to a radical proposed to undergo epoxide formation (Wennberg et al., 2018); we neglect this very minor and uncertain pathway as the product was suggested to be due to an impurity (St. Clair et al., 2016). "

p32 L1: Here you state that H-abstraction from the carbon dominates, but with a higher

C8

yield of HCHO than HCOOH, the former of which is derived from H-abstraction from the hydroperoxide, isn't that backwards? Also, within their reported uncertainty, Allen et al. (2018) did not conclusively state that one path dominates over the other.

We thank the Reviewer for spotting this mistake. The text has been changed as follows: "H-abstraction from hydroperoxide group, followed by decomposition of the hydroxymethylperoxy radical, is slightly dominant (Allen et al., 2018). H-abstraction from the carbon is followed by OH expulsion."

p32 L3: "he" should be "the"

Corrected.

p32 L5: the discussion here seems more suited for a subsection of section 2 than for a note at the bottom of a table; the generic monoterpene oxidation scheme provided here needs more discussion of its uncertainties and how the specific numbers were arrived at. While the complexity of terpene oxidation and the relative lack of quantitative knowledge about its oxidation mechanism make drastic simplification a necessity, it is not clear to the reader why this particular set of simplifications is ideal, or what the reasonable uncertainty bounds are on any of these rates and product yields. If pinene (or generic terpene) oxidation is to be included in this model, it should be given more than a paragraph in a footnote. The same might be said for MBO, but the relative simplicity of its oxidation mechanism, the overlap with isoprene oxidation products, and the smaller magnitude of its emissions make it less prone to substantial uncertainty and bias from mechanistic simplifications and shortcuts. Maybe some sensitivity studies showing the range of results you could get in a global model given the uncertainties in this mechanism would be most useful? (e.g. assuming more or less of the products are lost to SOA/deposition, or assuming a range of nitrate and/or HOx yields). Some specific questions include: on line 10, where does the 45% number come from? How do these simulated acetone and formaldehyde yields compare to previous work? What

C9

does this mechanism inherently assume for the SOA formation from pinene, and how does that compare to both measured yields and the magnitude of SOA formed from isoprene globally? What might be the implications in a global simulation of skipping oxidative steps (and therefore likely sinks of OH, HO₂, NO) in the oxidation mechanism, as is presumably the case when only one generation of products are used?

We moved this discussion to a new subsection (Section 2.4). As noted by the Reviewer, drastic simplification of the monoterpene mechanism is a necessity. We now better emphasize the limited scope of our simple mechanism, which is the reproduction of the final yields of a few key products. The subsection text is as follows:

"Due to the complexity and poor understanding of monoterpene oxidation, we adopt a simple parameterization based on box model simulations of α - and β -pinene oxidation using the MCMv3.2 (Saunders et al., 2003). The scope of the parameterization is limited to the reproduction of total yields of several key products; those yields reflect not only primary production but also secondary formation. The influence of monoterpenes on radicals (e.g. HO_x, RO₂) and on ozone production is therefore likely not well represented by this simple mechanism. It should be stressed that even the monoterpene mechanism in MCM is greatly oversimplified, as it neglects many possibly important pathways (in particular H-shift isomerisations in peroxy radicals), with potentially very large effects on radicals and other products. A thorough evaluation of mechanisms against laboratory data will be needed in order to assess their uncertainties, but is out of scope of the present study.

The parameterization relies on sixty-day simulations performed using the Kinetic Pre-Processor (KPP) package (Damian et al., 2002). The photolysis rates are calculated for clear-sky conditions at 30°N on July 15th. Although both high-NO_x (1 ppbv NO_x, 40 ppbv O₃ and 250 ppbv CO maintained throughout the simulation) and low-NO_x simulations (100 pptv NO_x, 20 ppbv O₃ and 150 ppbv CO) are conducted, only the low-NO_x results are used for the parameterization. Temperature and H₂O are kept at 298 K

C10

and 1% v/v. To determine the product yields, counter compounds are introduced in the equation file (e.g. HCHO_a, MGLYO_a, etc.) having the same production terms as the species they represent, but without any chemical loss.

The yield of acetone from both α - and β -pinene is very close to 100% after several days of reaction, independent of the NO_x level. The yield of methylglyoxal is low (4% and 5% for α - and β -pinene, not counting the contribution of acetone oxidation by OH). The overall yield of formaldehyde obtained in these simulations is \sim 4.2 HCHO per monoterpene oxidized, almost independent of NO_x, for both precursors. The HCHO yield comes down to 2.3 after subtracting the contributions of acetone and methylglyoxal oxidation. This yield is further reduced by 45% to account for wet/dry deposition of intermediates and secondary organic aerosol formation. That fraction is higher, but of the same order, as the estimated overall impact of deposition on the average formaldehyde yield from isoprene oxidation (\sim 30%), based on global model (MAGRITTE) calculations. The higher fraction is justified by the larger number of oxidation steps and the generally lower volatility of intermediates involved in formaldehyde formation from monoterpene oxidation. Nevertheless, this adjustment introduces a significant uncertainty in the model results. A sensitivity calculation shows that adopting a lower yield reduction (20% instead of 45%) in the global model (Sect. 4.1) has negligible impact on the calculated HCHO abundances ($<\sim$ 1%) in most regions, but leads to higher HCHO vertical columns in monoterpene emission regions, by \sim 5% over Amazonia and by up to 8% over Siberia. The associated impact on OH reaches +2% in those regions, due to the additional HO_x formation through HCHO photolysis.

The overall carbon balance of monoterpene oxidation in the mechanism is \sim 50% due to the combined effects of deposition, SOA formation and CO and CO₂ formation besides their production through the degradation of the explicit products. "

To our understanding, the assessment of uncertainties requested by the Reviewer is currently out of reach, in absence of any reliable reference mechanism validated by laboratory data. Note that the mechanism does not make specific assumption regard-

C11

ing SOA formation, besides the fact that it is expected to remove HCHO precursors from the gas-phase, and therefore reduce the overall HCHO yield.

p37 L14: How is the oxidative degradation of anthropogenic NMVOCs treated in the model? I am particularly concerned about the possible contribution of degradation of non-isoprene compounds to the gas-phase budgets of glyoxal and the organic acids. Along those same lines, could some discussion of the potential for additional sources of the gas-phase organic acids not included in this model (e.g. degradation of other compounds, revolatilization from SOA) be added to those sections?

The chemical oxidation mechanism of anthropogenic and biomass burning VOCs has been described in previous publications with the IMAGES model, as now mentioned in the model description (Section 4.1). The yields of glyoxal in the oxidation of aromatic compounds and acetylene are now provided in Section 4.5: "The glyoxal yields in their reactions with OH (0.74, 0.7, 0.36 and 0.636 for benzene, toluene, xylenes and acetylene, respectively) are obtained from the MCM (Saunders et al., 2003; Bloss et al., 2005). Regarding aromatics, this yield includes not only primary formation but also later-generation production (Chan Miller et al., 2016)." Since the topic of our study is the oxidation mechanism of biogenic VOCs, we don't believe necessary to lengthen the paper with more details on the chemistry of other VOCs.

We now include a short discussion of potential additional sources of formic and acetic acids at the end of Section 4.4: "Additional sources are likely at play, such as enol formation through other pathways than those considered here (e.g. in monoterpene and anthropogenic VOC oxidation, e.g. through the photolysis of aldehydes (Tadic et al., 2001a; Tadic et al., 2001b)) and the photodegradation of organic aerosols (Paultot et al., 2011; Malecha and Nizkodorov, 2016)."

p37 L18: Are there primary emissions of MBO in the model? What is the effect of the MBO oxidation mechanism (and the terpene mechanism) in the model?

C12

The global biogenic emissions of MBO amount to 0.93 TgC yr⁻¹. This is now mentioned in the model description section. The effect of MBO is small, due to its low emissions. Its oxidation is a source of acetone (~0.5 TgC yr⁻¹).

Monoterpenes have multiple, but very uncertain effects. The comparison of model simulations performed with and without monoterpene emissions indicates significant increases of several compounds due to monoterpenes, e.g. glyoxal (global burden +22%), acetone (+40%), acetic acid (+9%), formic acid (+12%) and formaldehyde (+3%). Much larger impacts are calculated over emission regions, e.g. HCHO vertical columns are increased by up to 15-20% over boreal forests and Amazonia. As monoterpene chemistry is by far the most uncertain part of the BVOC mechanism, we prefer not to discuss these impacts in the article, which is already very long.

p40 L5: In the comparisons to SEAC4RS data, it would be helpful to list the measurement uncertainties and spreads alongside the over/underestimations of the model. Also, what exactly is the model output being compared with the measurements in this section? Are the simulated average profiles just the average over the entire SE USA between 0900 and 1700 hours, or are they points subsampled from the model concurrent with the flight paths? If it's the former, which assumes that the SEAC4RS observations (masked for plumes and stratospheric intrusions) are representative of the averaged regions, how might this skew the comparison between the model and measurements?

The model profiles are averages based on values interpolated at each measurement location and time. This is now mentioned in the manuscript. Wherever relevant, measurement uncertainties and model over/underestimations are reported in the text. We don't believe especially helpful to make the paper longer with a new Table providing comparison statistics and measurement uncertainties.

p41 L5: Are these non-HPALD compounds also isoprene products? Do we have any indication as to what they are? If they have the same mass as the HPALDs, are there

C13

other species in your mechanism that also have this mass that may account for this mass?

Yes, the isoprene carbonyl hydroxy epoxides (ICHE) formed mainly from the oxidation of IEPOX by OH have the same formula ($C_5H_8O_3$) as HPALD. We now present a model comparison with the SEAC4RS measurement for that mass (Fig. 9). The following text accompanies this comparison: "The model-calculated HPALD concentrations (dotted line on the $C_5H_8O_3$ panel of Fig. 9) are on average about a factor of two lower than the observed Caltech CIMS (Chemical Ionisation Mass Spectrometry) signal at the corresponding mass; when adding the contribution of the carbonyl hydroxyepoxides (ICHE), which have the same formula ($C_5H_8O_3$) as HPALD and can be expected to interfere with HPALD measurements, the model falls within the measurement uncertainty (50%) with an underestimation decreased to -34% (solid line on Fig. 9). The ICHE compounds are formed from the oxidation of IEPOX (as well as HPALDs) by OH. It is likely than other, unknown compounds contribute to the CIMS signal at the same mass, as also observed in the PROPHET campaign in Michigan, where the HPALD contribution to the CIMS measurement at the given mass was estimated at 38% based on the relative contribution of the HPALD peaks to the total GC area (Vasquez et al., 2018). This is consistent with our modelled HPALD accounting for 50% of the CIMS measurement, when considering also that all isoprene oxidation products appear slightly overestimated by the model as suggested by the ~20% overprediction of modelled ISOPOOH and MVK+MACR relative to the measurements. In spite of the important uncertainties and remaining unknowns (e.g. the identity of additional compounds contributing to the CIMS signal), this good consistency provides strong support to the high HPALD yield (75%) adopted in this work in the isomerisation of *Z*- δ -OH-peroxys from isoprene (Sect. 2.1.2). Lower yield values as proposed in recent previous work, i.e. 50% (Peeters et al., 2014; Jenkin et al., 2015) or 25% (Teng et al., 2017; Wennberg et al., 2018) would lead to much stronger HPALD underestimations against SEAC⁴RS data. "

C14

Section 2.1.2 Products from the isomerization of the *Z*- δ -OH-peroxys

The 1,6 H-shift of the *Z*- δ -OH-peroxys $\text{HOCH}_2\text{C}(\text{CH}_3)=\text{CH}-\text{CH}_2\text{O}_2$ (Case I) and $\text{O}_2\text{CH}_2\text{C}(\text{CH}_3)=\text{CH}-\text{CH}_2\text{OH}$ (Case II) forms allylic radicals, e.g. $\text{Z}-\text{HOC}^\circ$ $\text{H}-\text{C}(\text{CH}_3)=\text{CH}-\text{CH}_2\text{OOH} \rightleftharpoons \text{Z}-\text{HOCH}=\text{C}(\text{CH}_3)=\text{C}^\circ\text{H}-\text{CH}_2\text{OOH}$ for Case I. Therefore, two second-generation peroxyxs can result, peroxy *i* ($\text{Z}-\text{HOCH}(\text{O}_2)\text{C}(\text{CH}_3)=\text{CH}-\text{CH}_2\text{OOH}$) and peroxy *ii* ($\text{Z}-\text{HOCH}=\text{C}(\text{CH}_3)\text{CH}(\text{O}_2)\text{CH}_2\text{OOH}$), in an approximate ratio of 40:60, and two pathways are open to product formation (Peeters et al., 2014). The subsequent chemistry is given here for Case I, unless stated otherwise. Peroxy *i* readily eliminates HO_2 at a rate of $\sim 2000 \text{ s}^{-1}$ (Hermans et al., 2005) to produce $\text{Z}-\text{O}=\text{CH}-\text{C}(\text{CH}_3)=\text{CH}-\text{CH}_2\text{OOH}$ (HPALD1) (Peeters et al., 2014; Peeters et al., 2009; Crounse et al., 2011; Teng et al., 2017). Peroxy *ii* may isomerise by a fast 1,6 enol-H-shift, promptly at $\sim 1.5 \cdot 10^9 \text{ s}^{-1}$ and thermally at $> 10^4 \text{ s}^{-1}$, to form $\text{Z}-\text{O}=\text{CH}-\text{C}^\circ(\text{CH}_3)\text{CH}(\text{OOH})\text{CH}_2\text{OOH}$ (Peeters and Nguyen, 2012; Peeters et al., 2014) that in part arises chemically activated such that it can promptly undergo concerted OH-loss and ring-closure to an hydroperoxy-carbonyl epoxide $\text{Z}-\text{HOOCH}_2-\text{C}(\text{HOC}(\text{CH}_3)\text{CHO})$ (HPCE), as proposed and observed by Teng et al. (2017), and for another part lead to a third-generation peroxy, $\text{Z}-\text{O}=\text{CH}-\text{C}(\text{CH}_3)(\text{O}_2)\text{CH}(\text{OOH})\text{CH}_2\text{OOH}$ (DIHPCARP1) (Peeters et al., 2014). The DIHPCARP radicals were suggested (Peeters et al., 2014) to either undergo a fast aldehyde-H-shift and eliminate CO and expel OH to form dihydroperoxy carbonyls, or react with NO and HO_2 , to result mainly in $\text{OH} + \text{CH}_3\text{C}(\text{O})\text{CHO}$ (MGLY) + HOOCH_2CHO (HPAC) (Case I), or $\text{OH} + \text{OCHCHO} + \text{CH}_3\text{C}(\text{O})\text{CH}_2\text{OOH}$ (HPACET) (Case II). While the CO elimination above may be fast enough to outrun O_2 addition for Case I (Novelli et al., 2018b), this appears less likely for Case II, for which the barrier should be about 2 kcal mol $^{-1}$ higher (Méreau et al., 2001). Note that HPAC

C15

and HPACET were observed by Teng et al., but in a ratio to HPALDs nearly independent of the NO level. Secondly, it is estimated using statistical rate theory that the 1,6 enol-H-shift above can occur for about half while its peroxy precursor is still chemically activated such that the resulting radical contains close to 30 kcal mol $^{-1}$ internal energy (Peeters et al., 2014), sufficient for prompt HPCE epoxide formation.

In this work, the quantitative product distribution from the 1,6 H-shift of the *Z*- δ -OH-peroxys is adopted from the recent experimental study of Berndt et al. (2019), supported and complemented by computational results of the LIM1 paper (Peeters et al., 2014). Note that the 1,6 H-shifts of the *Z*- δ -OH-peroxys occur for $\sim 85\%$ by tunneling (Coote et al., 2003) at energies lower than 2 kcal mol $^{-1}$ below the barrier top, such that the Boltzmann population there is only marginally affected by the O_2 -loss that occurs only at energies above this range; therefore there is no reason to suspect (Wennberg et al., 2018) that the agreement between experimental results (Teng et al., 2017) and the TST-predicted rate constants of Peeters et al. (2014) is fortuitous. The Berndt et al. investigation offers several advantages: (i) the reaction time was so short (8 s) that no secondary products could be formed; (ii) due to the absence of NO and near-absence of HO_2 , essentially only the products of the *Z*- δ -OH-peroxy 1,6 H-shift could be formed, so excluding potential interferences; (iii) the peroxy radicals could also be observed; (iv) the sampled products and peroxy radicals could be quasi-quantitatively converted into ion-complexes, detected by high-resolution mass spectrometry capable of measuring concentrations as low as 10^4 cm^{-3} . Hydroxyl radicals were prepared by reacting 10^{12} cm^{-3} of O_3 with $2 \cdot 10^{11} \text{ cm}^{-3}$ of tetramethylethylene, in presence of $2.5 \cdot 10^{12} \text{ cm}^{-3}$ of isoprene. At 8 s reaction time, the modeled total ISOPOO concentration is $1.2 \cdot 10^9 \text{ cm}^{-3}$, of which $6 \cdot 10^6 \text{ cm}^{-3}$ *Z*- δ -OH-peroxys (50% Case I isomer $\text{HOCH}_2\text{C}(\text{CH}_3)=\text{CHCH}_2\text{O}_2$, and 50% Case II isomer $\text{O}_2\text{CH}_2\text{C}(\text{CH}_3)=\text{CHCH}_2\text{OH}$ at 8 s). Integrated over the entire reaction time of 8 s, the modeled ratio of these two peroxyxs is circa 0.8:1.0. Using the isomer-specific 1,6 H-shift rates of 0.36 s^{-1} and 3.7 s^{-1} for *Z*- δ -OH-peroxys I and II (Teng et al., 2017), the expected total formation rate of isomerization products at 8 s is $1.2 \cdot 10^6 \text{ cm}^{-3} \text{ s}^{-1}$. For these conditions, Berndt et

C16

al. measured the following concentrations at 8 s: $C_5H_8O_3$ (HPALDs): $2.3 \cdot 10^7 \text{ cm}^{-3}$; $C_5H_8O_4$ (hydroperoxy carbonyl epoxides): $4.6 \cdot 10^6 \text{ cm}^{-3}$; $C_4H_8O_5$ (dihydroperoxy carbonyls): $6.2 \cdot 10^5 \text{ cm}^{-3}$; $C_5H_9O_5$ (the second-generation peroxy above): $1.7 \cdot 10^6 \text{ cm}^{-3}$; and $C_5H_9O_7$ (the third-generation peroxy): $3.5 \cdot 10^5 \text{ cm}^{-3}$. In principle, these values are minimum concentrations. No HPAC nor HPACET was detected. The detected product and peroxy concentrations account together for 60% of the modeled total products at 8 s using the experimental kinetic parameters of Teng et al., which, together with the uncertainties, leaves room for some other products. The theoretically derived parameters of Peeters et al. (2014) predict a higher product formation from the Z - δ -OH-peroxy isomerization at 8 s, but this is due to a too low LIM1-predicted O_2 -loss from the peroxy, such that the populations of the Z - δ -OH-peroxy at 8 s are still too close to their high initial formation fraction and attain their much lower final steady-state fraction too late.

The Berndt et al. results thus give the following product yields at 8 s: HPALDs: 76%; HPCE: 15%; dihydroperoxy carbonyls: 2%; while 5.5% of the reacted Z - δ -OH-peroxy is present as second-generation peroxy $C_5H_9O_5$ and 1% as third-generation peroxy $C_5H_9O_7$. The HPALD yield determined by Berndt et al. is much higher than that of Teng et al. However, another, non-HPALD, $C_5H_8O_3$ compound observed by Teng et al. could be speculated to be a perhemiketale formed from HPALDs on the walls of the 1 m sampling tubing. Another observation of Berndt et al. indirectly supports a high HPALD yield. The concentration of the second-generation peroxy is strikingly high, given that the peroxy of type *i* are expected to react at a rate of $\sim 2000 \text{ s}^{-1}$ and those of type *ii* even at $> 10^4 \text{ s}^{-1}$, such that at the given Z - δ -OH-peroxy concentrations, and using the experimental 1,6 H-shift rates for Z - δ -OH-peroxy I and II, they should be present in a quasi-steady-state concentration of only about 10^4 cm^{-3} . This indicates that a large fraction of the $C_5H_9O_5$ peroxy are Z, E' - $\text{HOCH}=\text{C}(\text{CH}_3)\text{-CH}(\text{O}_2)\text{-CH}_2\text{OOH}$ isomers of peroxy *ii* (and similar for Case II) with the OH pointing outwards, away from the peroxy function, such that they cannot undergo the 1,6 enol-H-shift, and can only be removed by (repeated) O_2 -loss and re-addition, to finally convert to Z, E' -

C17

$\text{HOCH}(\text{O}_2)\text{C}(\text{CH}_3)=\text{CHCH}_2\text{OOH}$ peroxy *i* that quickly expel HO_2 to form additional HPALDs. Such a high fraction of Z, E' peroxy *ii* is consistent with the computational results (Peeters et al., 2014) on the various transition states for the 1,6 H-shift of the Z - δ -OH-peroxy. For Case I, a Z, Z' -TS with the OH inward was found to account for about 67% of the rate and a Z, E' -TS with OH outward for 33%, while for Case II two Z, E' -TSs account for 69% and a Z, Z' -TS for 31% of the rate. For the conditions of Berndt et al. at 8 s, with the integrated 1,6 H-shift rate due for $\sim 92\%$ to the Case II- and for $\sim 8\%$ to the Case I- Z - δ -OH-peroxy, the weighted average is $\sim 65\%$ reaction through Z, E' - and 35% through Z, Z' -structures. Taken together, the above strongly suggests that, contrary to a speculative suggestion in the LIM1 paper, the $Z - E$ isomerism of the transition states is conserved in the allylic-radical products and in the resulting peroxy *i* and *ii*. A statistical rate estimate for the prompt internal rotation of the OH in the Z, E' -hydroxyl-allyl product radicals, with computed barrier 12 kcal mol^{-1} and imaginary frequency close to 100 cm^{-1} , and for a nascent vibration energy of 21 kcal mol^{-1} , predicts $k \sim 10^8 \text{ s}^{-1}$, or 10 times slower than collisional stabilization followed by O_2 -addition. Therefore, allowing for 10% internal rotation of the OH in the nascent Z, E' product isomers to form the more stable, H-bonded Z, Z' forms, about 40% of the allylic radicals and their O_2 -adducts would end up with the OH inwards and $\sim 60\%$ with the OH outwards in the Berndt et al. conditions. Further adopting also the spin densities in the allylic product radical of the LIM1 paper, i.e. 0.4 on carbon 1 and 0.6 on carbon 3 for Case I (and similarly 0.4 on carbon 4 and 0.6 on carbon 2 for Case II), as well as the corresponding 40:60 branching ratio for peroxy *i* and *ii* formation, the mechanism above would result in 40% direct formation of HPALDs through peroxy *i*, only 24% enol-H-shift products through Z, Z' peroxy *ii*, and 36% formation of the slowly reacting Z, E' peroxy *ii*, which in the Berndt et al. conditions would lead to ca. 31% indirect HPALD production through O_2 -loss and re-addition of the Z, E' peroxy *ii* to form peroxy *i*, while around 5% still survives as Z, E' peroxy *ii* in the short reaction time available. The so predicted overall 71% HPALD yield, based on computational results from the LIM1 paper, is strikingly close to the experimental yield of Berndt et al.

C18

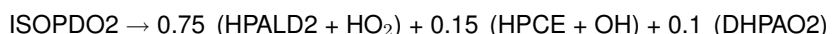
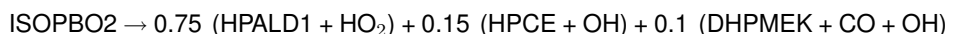
Moreover, at a total product formation rate of $1.2 \cdot 10^7 \text{ cm}^{-3} \text{ s}^{-1}$, the 31% contribution due to Z, E' peroxy *ii* reacting to HPALDs at 8 s implies a reaction rate of $3.8 \cdot 10^6 \text{ cm}^{-3} \text{ s}^{-1}$, or at the measured Z, E' -peroxy *ii* concentration of $1.7 \cdot 10^6 \text{ cm}^{-3}$, an effective rate constant of 2.2 s^{-1} . Since on average 2.5 cycles of O_2 -loss and re-addition are required to form HPALD from Z, E' peroxy *ii* through peroxy *i*, an O_2 -loss rate of 6 s^{-1} is derived, which is typical for hydroxy-allyl peroxys such as the very similar initial Z - and E - δ -OH-peroxys from isoprene (Teng et al., 2017).

The 15% HPCE yield measured by Berndt et al. is compatible with the product radical of the 1,6 enol-H-shift of Z, Z' -peroxy *ii* arising for a large fraction with sufficient chemical activation to overcome the barrier of ca. 15 kcal mol⁻¹ for the concerted ring-closure and OH loss. The theory-based 24% enol-H-shift products through peroxy *ii*, above, comprises the HPCE epoxides and products of the third-generation peroxys (DIHPCARP). Adopting the experimental 15% HPCE yield would leave room for some 10 % DIHPCARP-derived products, of which, apparently, the dihydroperoxy carbonyls account for only a small fraction of 2%. The minimum concentration of the DIHPCARPs in the Berndt et al. experiment is $3.5 \cdot 10^5 \text{ cm}^{-3}$, while their loss rate by aldehyde-H shift (followed by either CO elimination or O_2 -addition) should be about 2 s^{-1} according to Møller et al. (2019), and 6 s^{-1} according to Novelli et al. (2018c), such that their expected reaction rate is $0.7 \text{--} 2.1 \cdot 10^6 \text{ cm}^{-3} \text{ s}^{-1}$, or 6–18% of the overall products formation rate of $1.2 \cdot 10^7 \text{ cm}^{-3} \text{ s}^{-1}$ above. Subtracting the 2% dihydroperoxy carbonyls leaves 4–16 % going to other products, consistent with the ~8% estimated above, and in line with the expectation, in the introduction of this section, that the acyl product of aldehyde-H-shift in the most abundant DIHPCARP (Case II) does not eliminate CO but rather adds O_2 to continue the autoxidation chain by forming fourth-generation peroxy C₅H₉O₉, with HOOCH₂-C(CH₃)(O₂)-CH(OOH)-C(O)OOH (DHPAO2) likely the most stable isomer after fast hydroperoxide-H shifts (Jorgensen et al., 2016) because it allows three H-bonds of which two are synergic and therefore stronger (Dibble, 2004). Since (other) fast H-shifts for this isomer are not possible, it can only react with NO or HO₂. The main resulting oxy product radical should decompose rapidly (Vereecken et

C19

al., 2009) into HPACET + OH + OCHC(O)OOH.

In atmospheric conditions, the various peroxys are all in quasi-steady state, which means ~5% more HPALD production from the Z, E' -peroxys *ii*, and ~1% more DIHPCARP products than in the Berndt et al. conditions at 8 s. On the other hand, the atmospheric steady-state product formation ratio from the Z - δ -OH-peroxys Case I and Case II is rather 18:82, instead of the 8:92 ratio of the Berndt et al. experiment (Teng et al., 2017), such that about 43% of the second-generation radicals would end up with the OH inwards and ~57% with the OH outwards. Taking into account also the above, direct (40%) plus indirect (34%) HPALD formation would add up to 74%, while the expected HPCE yield is 16% and that of the DIHPCARP products around 10%, of which 2% the dihydroperoxy carbonyl DHPMEK. Acknowledging the large uncertainties in those yields, we represent the Z - δ -OH-peroxy isomerisations as



Here, HPCE is a mixture of 18% Case I and 82% Case II compounds. Its oxidation by OH proceeds mainly by aldehyde-H abstraction, forming a carbonyl radical; the same radical can also be formed through OH-abstraction of the hydroperoxide-H in HPCE, followed by a 1,6 aldehyde-H-shift. The carbonyl radical can undergo concerted CO elimination and ring opening, forming CH₃C(O)CH(O₂)CH₂OOH (for Case I) or OCHC(O₂)(CH₃)CH₂OOH (for Case II). The latter peroxy undergoes a 1,4 H-shift to CO + OH + CH₃C(O)CH₂OOH (HPACET). Such H-shift being not open for the Case I peroxy radical, it reacts primarily with NO or HO₂, leading for the most part to CH₃C(O)CH(O[°])CH₂OOH that promptly decomposes into either CH₃C(O) + OCH₂OOH (HPAC), or HCHO + OH + MGLY. Photolysis of HPCE can be expected

C20

to proceed by splitting off the formyl radical, leading to the same peroxy radicals as above.

References

Allen, H. M., Crounse, J. D., Bates, K. H., Teng, A. P., Krawiec-Thayer, M. P., Rivera-Rios, J. C., Keutsch, F. N., St. Clair, J. M., Hanisco, T. F., Moller, K. H., Kjaergaard, H. G., and Wennberg, P. O.: Kinetics and product yields of the OH initiated oxidation of hydroxymethyl hydroperoxide, *J. Phys. Chem. A*, 122, 6292–6302, 2018.

Berndt, T., Jokinen, T., Sipilä, M., Mauldin III, R. L., Herrmann, H., Stratmann, F., Junninen, H. and Kulmala, M.: H_2SO_4 formation from the gas-phase reaction of stabilized Criegee Intermediate with SO_2 : Influence of water vapour content and temperature, *Atmos. Environ.*, 89, 603–612, 2014.

Bloss, C., Wagner, V., JJenkin, M. E., Volkamer, R., Bloss, W. J., Lee, J. D., Heard, D. E., Witz, K., Martin-Reviejo, M., Rea, G., Wenger, J. C., and Pilling, M. J.: Development of a detailed chemical mechanism (MCMv3.1) for the atmospheric oxidation of aromatic hydrocarbons, *Atmos. Chem. Phys.*, 5, 641–664, 2005.

Compernolle, S., Ceulemans, K., and Müller, J.-F.: EVAPORATION: a new vapour pressure estimation method for organic molecules including non-additivity and intramolecular interactions, *Atmos. Chem. Phys.*, 11, 9431–9450, 2011.

C21

Coote, M. L., Collins, M. A., and Radom, L.: Calculation of accurate imaginary frequencies and tunneling coefficients for hydrogen abstraction reactions using IRCmax, *Mol. Phys.*, 101, 1329–1338, 2003.

Crounse, J. D., Paulot, F., Kjaergaard, H. G., and Wennberg, P. O.: Peroxy radical isomerization in the oxidation of isoprene, *Phys. Chem. Chem. Phys.*, 13, 13607–13613, 2011. Amendment: <http://www.rsc.org/suppdata/cp/c1cp21330j/addition.htm>.

Damian, V., Sandu, A., Damian, M., Potra, F., and Carmichael, G.: The Kinetic PreProcessor KPP – A software environment for solving chemical kinetics, *Comput. Chem. Eng.*, 26, 1567–1579, 2002.

D'Ambro, E. L., Møller, K. H., Lopez-Hilfiker, F. D., Schobesberger, S., Liu, J., Shilling, J. E., Kjaergaard, H. G., and Thornton, J. A.: Isomerization of second-generation isoprene peroxy radicals: Epoxide formation and implications for Secondary Organic Aerosol yields, *Environ. Sci. Technol.*, 51, 4978–7987, 2017.

D'Ambro, E., Schobesberger, S., Gaston, C. J., Lopez-Hilfiker, F., Lee, B. H., Liu, J., Zelenyuk, A., Bell, D., Cappa, C. D., Helgestad, T., Li, Z., Guenther, A., Wang, J., Wise, M., Caylor, R., Surratt, J. D., Riedel, T., Hyttinen, N., Salo, V.-T., Hasan, G., Kurtñ, T., Shilling, J. E., and Thornton, J. A.: Chamber-based insights into the factors controlling IEPOX SOA yield, composition, and volatility, *Atmos. Chem. Phys. Discuss.*, <https://doi.org/10.5194/gmd-11-3235-2018>, 2019.

Dibble, T. S.: Intramolecular hydrogen bonding and double H-Atom transfer in peroxy and alkoxy radicals from isoprene, *J. Phys. Chem. A*, 108, 2199–2207, 2004.

C22

Fu, T.-M., Jacob, D. J., Wittrock, F., Burrows, J. P., Vrekoussis, M., and Henze, D. K.: Global budgets of atmospheric glyoxal and methylglyoxal, and implications for formation of secondary organic aerosols, *J. Geophys. Res.*, 113, D15303, 2008.

Hermans, I., Muller, J.-F., Nguyen, T., Jacobs, P., and Peeters, J.: Kinetics of α -hydroxy-alkylperoxy radicals in oxidation processes. HO₂-Initiated oxidation of ketones/aldehydes near the tropopause, *J. Phys. Chem. A*, 109, 4303–4311, 2005.

Jenkin, M. E., Young, J. C. and Rickard, A. R.: The MCM v3.3.1 degradation scheme for isoprene, *Atmos. Chem. Phys.*, 15, 11433–11459, 2015.

Jørgensen, S., Knap, H. C., Otkjaer, R. V., Jensen, A. M., Kjeldsen, M. L. H., Wennberg, P. O., and Kjaergaard, H. G.: Rapid hydrogen shift scrambling in hydroperoxy-substituted organic peroxy radicals, *J. Phys. Chem. A*, 120, 266–275, 2016.

Lin, Y.-H., Zhang, Z., Docherty, K. S., Zhang, H., Budisulistiorini, S. H., Rubitschun, C. L., Shaw, S. L., Knipping, E. M., Edgerton, E. S., Kleindienst, T. E., Gold, A., and Surratt, J. D.: Isoprene epoxydiols as precursors to secondary organic aerosol formation: acid-catalyzed reactive uptake studies with authentic compounds, *Environ. Sci.*, 46, 250–258, 2012.

Malecha, K. T., and Niskodorov, S. A.: Photodegradation of secondary organic aerosol particles as a source of small, oxygenated volatile organic compounds, *Environ. Sci. Technol.*, 50, 9990–9997, 2016.

C23

Møller, K. H., Bates, K. H., and Kjaergaard, H. G.: The importance of peroxy radical hydrogen-shift reactions in atmospheric isoprene oxidation, *J. Phys. Chem. A*, 123, 920–930, 2019.

Müller, J.-F., Stavrakou, T., Bauwens, M., Compernolle, S., and Peeters, J.: Chemistry and deposition in the Model of Atmospheric composition at Global and Regional scales using Inversion Techniques for Trace gas Emissions (MAGRITTE). Part B. Dry deposition, submitted to *Geophys. Model Dev. Discuss.*, 2018.

Novelli, A., Bohn, B., Dorn, H. P., Hofzumahaus, A., Holland, F., Li, X., Kaminski, M., Yu, Z., Rosanka, S., Reimer, D., Gkatzelis, G. I., Taraborrelli, D., Vereecken, L., Rohrer, F., Tillmann, R., Wegener, R., Kiendler-Scharr, A., Wahner, A., and Fuchs, H.: The atmosphere of a tropical forest simulated in a chamber: experiments, theory and global significance of OH regeneration in isoprene oxidation, iCACGP-IGAC 2018 Conference, Takamatsu, Japan, 2018b.

Novelli, A., Vereecken, L., Bohn, B., Dorn, H.-P., Hofzumahaus, A., Holland, F., Li, X., Kaminski, M., Yu, Z., Rosanka, S., Reimer, D., Gkatzelis, G. I., Taraborrelli, D., Rohrer, F., Tillmann, R., Wegener, R., Kiendler-Scharr, A., Wahner, A., and Fuchs, H.: The impact of the aldehyde-hydrogen shift on the OH radical budget in the isoprene oxidation mechanism in pristine environments, Atmospheric Chemical Mechanism (ACM) Conference, Davis, Dec. 2018.

Peeters, J., Nguyen, T. L. and Vereecken, L.: HOx radical regeneration in the oxidation of isoprene, *Phys. Chem. Chem. Phys.*, 11, 5935–5939, 2009.

Peeters, J., and Nguyen, T. L.: Unusually fast 1,6-H shifts of enolic hydrogens in

C24

peroxy radicals: formation of the first-generation C₂ and C₃ carbonyls in the oxidation of isoprene, *J. Phys. Chem. A*, 116, 6134–6141, 2012.

Peeters, J., Müller, J.-F., Stavrakou, T., and Nguyen, S. V.: Hydroxyl radical recycling in isoprene oxidation driven by hydrogen bonding and hydrogen tunneling: the upgraded LIM1 mechanism, *J. Phys. Chem. A*, 118, 8625–8643, 2014.

Pugh, T. A. M., MacKenzie, A. R., Langford, B., Nemitz, E., Misztal, P. K., and Hewitt, C. N.: The influence of small-scale variations in isoprene concentrations on atmospheric chemistry over a tropical rainforest, *Atmos. Chem. Phys.*, 11, 4121–4134, 2011.

Saunders, S. M., M. E. Jenkin, R. G. Derwent, and M. J. Pilling: Protocol for the development of the Master Chemical Mechanism, MCM v3 (Part A): tropospheric degradation of non-aromatic volatile organic compounds, *Atmos. Chem. Phys.*, 3, 161–180, 2003.

Stadtler, S., Kühn, T., Schröder, S., Taraborrelli, D., Schultz, M. G., and Kokkola, H.: Isoprene-derived secondary organic aerosol in the global aerosol-chemistry-climate model ECHAM6.3.0-HAM2.3-MOZ1.0, *Geosci. Model Dev.*, 11, 3235–3260, 2018.

Stavrakou, T., Müller, J.-F., De Smedt, I., Van Roozendael, M., Kanakidou, M., Vrekoussis, M., Witrock, F., Richter, A., Burrows, J. P.: The continental source of glyoxal estimated by the synergistic use of spaceborne measurements and inverse modelling, *Atmos. Chem. Phys.*, 9, 8431–8446, 2009b.

C25

St. Clair, J. M., Rivera-Rios, J., Crounse, J. D., Knap, H. C., Bates, K. H., Teng, A. P., Jørgensen, S., Kjaergaard, H. G., Keutsch, F. N., and Wennberg, P. O.: Kinetics and products of the reaction of the first-generation isoprene hydroxy hydroperoxide (ISOPOOH) with OH, *J. Phys. Chem. A*, 120, 1441–1451, 2016.

Surratt, J. D., Chan, A. W. H., Eddingsaas, N. C., Chan, M., Loza, C. L., Kwan, A. J., Hersey, S. P., Flagan, R. C., Wennberg, P. O., and Seinfeld, J. H.: Reactive intermediates revealed in secondary organic aerosol formation from isoprene, *Proc. Nat. Acad. Sci.*, 107, 6640–6645, 2010.

Tadic, J., Juranic, I., and Moortgat, G. K.: Pressure dependence of the photooxidation of selected carbonyl compounds in air: n-butanal and n-pentanal, *J. Photochem. Photobiol. A*, 143, 169–179, 2001a.

Tadic, J., Juranic, I., and Moortgat, G. K.: Photooxidation of n-hexanal in air, *Molecules*, 6, 287–299, 2001b.

Teng, A. P., Crounse, J. D., Lee, L., St. Clair, J. M., Cohen, R. C., and Wennberg, P. O.: Hydroxy nitrate production in the OH-initiated oxidation of alkenes, *Atmos. Chem. Phys.*, 15, 4297–4316, 2015.

Vasquez, K. T., Allen, H. M., Crounse, J. D., Praske, E., Xu, L., Noelscher, A. C., and Wennberg, P. O.: Low-pressure gas chromatography with chemical ionization mass spectrometry for quantification of multifunctional organic compounds in the atmosphere, *Atmos. Meas. Tech.*, 11, 6815–6832, 2018.

C26

Vereecken, L., and Peeters, J.: Decomposition of substituted alkoxy radicals - part I: a generalized structure-activity relationship for reaction barrier heights, *Phys. Chem. Chem. Phys.*, 11, 9062–9074, 2009.

Wennberg, P. O., Bates, K. H., Crounse, J. D., Dodson, L. G., McVay, R., Mertens, L. A., Nguyen, T. B., Praske, E., Schwantes, R. H., Smarte, M. D., St Clair, J. M., Teng, A. P., Zhang, X., and Seinfeld, J. H.: Gas-phase reactions of isoprene and its major oxidation products, *Chem. Rev.*, 118, 3337–3390, 2018.

Interactive comment on *Geosci. Model Dev. Discuss.*, <https://doi.org/10.5194/gmd-2018-316>, 2018.